

MODE COMPONENT EVOLUTION AND COHERENCE ANALYSIS IN TERAWATT TAPERED FEL

K. Fang, S.D. Chen, X. Huang, C. Pellegrini, J. Wu, SLAC, CA 94025, USA

K. Fang, Indiana University, IN 47405, USA

C. Emma, C. Pellegrini, University of California, Los Angeles, CA 90095, USA

S.D. Chen, C.S. Hwang, NCTU, Hsinchu 30076, Taiwan

S. Serkez, Deutsches Elektronen-Synchrotron, 22607 Hamburg, Germany

Abstract

A fast and robust algorithm is developed to decompose FEL radiation field transverse distribution into a set of orthonormal basis. Laguerre Gaussian and Hermite Gaussian can be used in the analysis. The information of mode components strength and Gaussian beam parameters allows users in downstream better utilize FEL. With this method, physics of mode components evolution from starting stage, to linear regime and post saturation are studied with detail. With these decomposed modes, correlation function can be computed with less complexity. Eigenmodes of the FEL system can be solved using this method.

INTRODUCTION

Free Electron Laser (FEL) is a powerful source that generates high brightness radiation for scientific research. Radiation at TW level may be able to resolve a single molecule image [1,2]. One way to improve brightness is to increase total photon number by tapering the undulator. This scheme has been proposed in [3], Now it is arousing the FEL community's interest [4,5]. Recently the effect different transverse electron distributions on taper efficiency is also studied.

The transverse content for a radiation is an important property of FEL. It may provide useful information in the down stream. Also as it's pointed out in [5], the transverse content plays an important role in tapered FEL. This paper may provide insight into transverse content by decomposing electric field transverse distribution generated from Genesis 1.3 [6] into Hermite Gaussian modes. With this decomposition, correlation function can be computed with less effort. Moreover, this method also provides a tool to study eigenmodes of the FEL system.

MODE DECOMPOSITION METHOD

In this study we decompose electric field into a set of Hermite Gaussian modes. Hermite Gaussian modes is a set of orthonormal basis. Two dimensional Hermite Gaussian modes allows x and y directions to have different distributions. The transverse radiation field along the undulator can be written as

$$E(\mathbf{r}; z) = \sum a_{mn}(z) H_m\left(\frac{\sqrt{2}}{w(z)}x\right) H_n\left(\frac{\sqrt{2}}{w(z)}y\right) \exp(-\zeta r^2). \quad (1)$$

Here $\zeta_r = \frac{1}{w^2}$, $\zeta_i = \frac{k}{2R}$. w is the spot size of fundamental Gaussian mode, while R describes the wave front curvature.

In this work, we use orthogonal condition to find amplitude a_{mn} for each Hermite-Gaussian mode. Wavefront curvature need to be eliminated before applying the orthogonal condition. To fit R , a lens with focal length f is applied to electric field. Then beam waist of the modified field is found through propagation. Curvature radius is found when the spot size of modified electric field diverges in both forward and backward propagation. After eliminating wavefront curvature, orthogonal condition is applied to extract mode amplitudes.

$$a_{mn} = \int E(\mathbf{r}; z) H_x\left(\frac{\sqrt{2}}{w}x\right) H_y\left(\frac{\sqrt{2}}{w}y\right) \exp(-\zeta r^2). \quad (2)$$

This integral has to be evaluated in a discrete form with finite cutoff, nevertheless good accuracy can still be achieved when w falls in some range.

To test the orthogonality, we define a matrix elements

$$C_{ij} = \sum_q H_m\left(\frac{\sqrt{2}x_q}{w}\right) H_n\left(\frac{\sqrt{2}y_q}{w}\right) H_k\left(\frac{\sqrt{2}x_q}{w}\right) H_l\left(\frac{\sqrt{2}y_q}{w}\right) \exp(-\zeta r_q^2) \frac{2\Delta x \Delta y}{w^2}, \quad (3)$$

where i and j has one to one correspondence with (m, n) and (k, l) . Fig. 1 describes how the orthogonality is maintained in this numerical method. In the region where w is small, there is not enough sampling rate to resolve structures in Hermite Gaussian modes. Therefore orthogonality condition is degraded. In large w region, numerical integral is inaccurate because of the cutoff error. Numerical integral could provide accurate expansion for electric field in basis with moderate w . To expand electric field in w where orthogonality condition is not preserved, we could first expand electric field with moderate w . Then expansion in other parameter w' can be computed by transformation method. The amplitudes in w' basis are connected with amplitudes in w basis with

$$a_{mn}(w') = \sum_{k,j} T_{m,k}(w'|w) T_{n,j}(w'|w) a_{kj}(w). \quad (4)$$

Here $T_{m,k}(w'|w) = \int H_m\left(\frac{\sqrt{2}}{w'}x\right) H_k\left(\frac{\sqrt{2}}{w}x\right) \exp\left(-\frac{x^2}{w'^2} - \frac{x^2}{w^2}\right) dx$.

Electric field can be decomposed into Hermite-Gaussian modes along the undulator in a tapered FEL. Yet, there

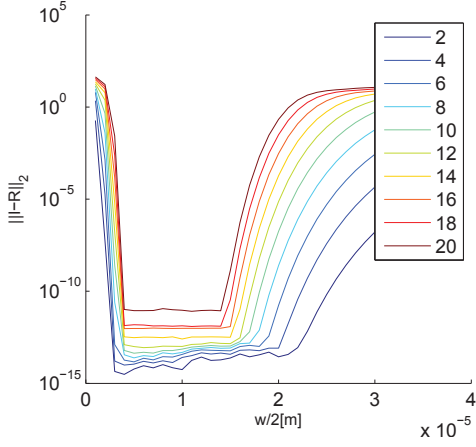


Figure 1: Figure plots how $R = \|I - C\|_2$ varies with w for general FEL simulation condition. 191 grid points are evenly distributed within a $[-180\mu\text{m}, 180\mu\text{m}]$ window in both directions. Different color corresponds to different maximal index number. For example, $N = 4$ corresponds to 16 modes with index $0 \leq m, n \leq 3$.

is free parameter w needs to be determined, for Hermite-Gaussian is a complete set of basis for different w . In linear regime, $w(z)$ describes the Gaussian mode that has the strongest coupling to the electrons, i.e. electric mode that has maximal growth rate. And in this regime, $w(z)$ can be computed using 3D FEL theory, e.g. [7]. In this work, we are going to obtain $w(z)$ by maximizing fundamental mode power. The same method can then be extended to post saturation regime where 3D theory is hard to solve. Fig. 2 plots the power of high order modes $\kappa = \sum_{mn \neq 0} |a_{mn}|^2 / |a_{00}|^2$ as a function of w at different locations of the undulator. κ for different locations have similar dependency on w , i.e. there is a w that could minimize κ . This could be explained as follows. For electric field with some radiation size σ_r , it can be described by fewer terms in Hermite-Gaussian basis with $w \approx 2\sigma_r$ than other w . For case w is significantly larger than $2\sigma_r$, high order modes are added destructively to construct the electric field. For case w is significantly smaller than $2\sigma_r$, high order modes are added constructively.

At the early stage of FEL process, about half of the FEL power is in the high order modes (minimal κ for $L = 10m$). This may also be seen from some structures in the core of the electric field distribution (Fig. 3). These structures indicate the existence of high order mode component. And the decomposition result (Fig. 4) is able to reconstruct these structures. High portion of high order mode is a result of the fact that the input seed is not the eigenmodes of the FEL interaction. Therefore it couples to many high order mode components. And as the FEL interaction proceeds, the fundamental mode, with the highest grow rate, starts to dominate. About 90% of the power is in the fundamental mode when FEL reaches saturation at $z = 30m$ (Fig. 2). As FEL interaction proceeds further into post saturation, high

order mode components start to increase, i.e. κ function has higher minimal value after saturation point after $30m$.

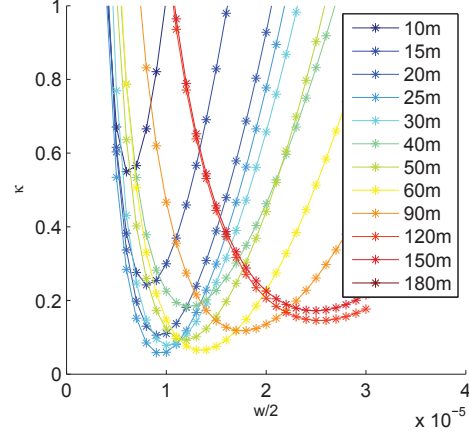


Figure 2: Here plots the total power of all the high order modes for different w . We choose w such $\kappa = \sum_{mn \neq 0} |a_{mn}|^2 / |a_{00}|^2$ is minimized.

COHERENCE ANALYSIS

With the decomposed electric field, coherence function can be computed with less effort.

$$\Gamma(\mathbf{r}_1, \mathbf{r}_2) = \frac{\langle E(\mathbf{r}_1)E^*(\mathbf{r}_2) \rangle}{\sqrt{\langle |E(\mathbf{r}_1)|^2 \rangle \langle |E(\mathbf{r}_2)|^2 \rangle}} \quad (5)$$

Then the time average can be computed as,

$$\begin{aligned} \langle E(\mathbf{r}_1)E^*(\mathbf{r}_2) \rangle &= \sum \langle a_{mn}a_{pq}^* \rangle H_m\left(\frac{\sqrt{2}}{w}x_1\right)H_n\left(\frac{\sqrt{2}}{w}y_1\right) \\ &H_p\left(\frac{\sqrt{2}}{w}x_2\right)H_q\left(\frac{\sqrt{2}}{w}y_2\right)\exp\left(-\frac{\mathbf{r}_1^2 + \mathbf{r}_2^2}{w^2}\right), \end{aligned} \quad (6)$$

where $\langle a_{mn}a_{pq}^* \rangle = \int a_{mn}(s)a_{pq}^*(s)ds$. The advantage of this method is that the ensemble average $\langle \dots \rangle$ only need to compute once.

Fig. 5 plots the one point correlation function, i.e. $\mathbf{r}_1 = 0$ in Eq. 5, in different regimes. At the beginning, only the central area has high correlation. As FEL process evolves, radiation field is diffracted from the center, therefore phase information is brought to the outer region. There is some ring structure in the correlation function. These structures come from the diffraction in the undulator gap. As FEL reaches post saturation regime, diffraction effect becomes even more important, resulting in a large coherent area.

MODE EVOLUTION

In FEL process, electric field evolution can be expressed as

$$\begin{aligned} \hat{O}_{FEL}(\Psi_1 + \Psi_s) &= \tilde{\Psi}_1 \\ &= \Psi_2 + \hat{O}_{FEL}\Psi_s. \end{aligned} \quad (7)$$

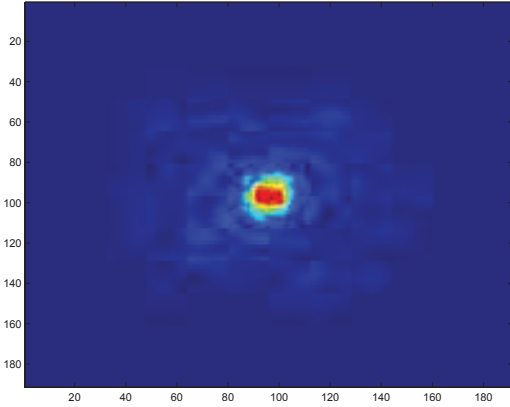


Figure 3: Electric field at 10m from Genesis simulation.

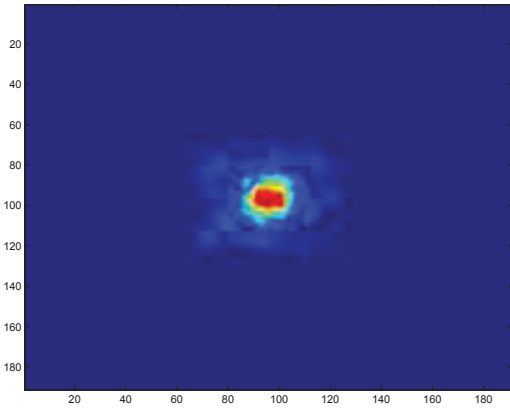
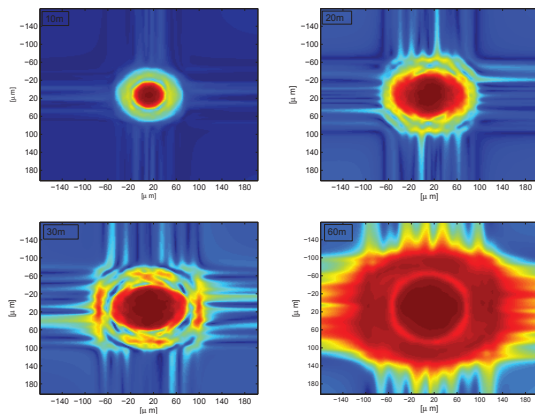
Figure 4: Reconstructed field from Hermite Gaussian modes, $E = \sum_{m,n=0} a_{mn} H_m\left(\frac{\sqrt{2}}{w}x\right) H_n\left(\frac{\sqrt{2}}{w}y\right) \exp\left(-\frac{x^2+y^2}{w^2}\right)$.

Figure 5: One point correlation function is plotted at different locations of the undulator. Four plots represent initial stages, linear regime, saturation and postsaturation respectively. Coherence area is increasing as FEL process proceeds.

Here $\Psi_{1,2}$ are the state of transverse distribution at two different locations, while Ψ_s represents the state accounting for bunching at location one. \hat{O}_{FEL} is a non self-adjoint linear operator that evolves electric field from location 1 to location 2. Genesis is used to compute this evolution. Transverse electric field distribution Ψ_1 interacts with particle distribution Ψ_s in Genesis. The output electric field $\hat{\Psi}_1$ is then a linear superposition of both Ψ_2 and $\hat{O}_{FEL}\Psi_s$. Therefore the evolved state Ψ_2 from Ψ_1 is computed by $\hat{\Psi}_1 - \hat{O}_{FEL}\Psi_s$, where $\hat{O}_{FEL}\Psi_s$ is computed by simulating by setting input radiation zero.

Our simulation scheme using Genesis is described as follows,

- Simulate FEL process through an Undulator section $U1$ with the output electric field transverse distribution E_1 and electron distribution $f_1(\vec{x})$.
- Decompose transverse profile E_1 into Hermite Gaussian modes $\{HG_n\}$.
- Simulate each Hermite Gaussian modes HG_n independently with electron distribution $f_1(\vec{x})$ for another section $U2$ with output field E_{2n} .
- Simulate electron beam $f(\vec{x})$ without electric field for $U2$ with output field E_b .
- HG'_n is then obtained by subtracting E_b from E_{2n} .

Fig. 6 plots the evolution of the first four Hermite Gaussian modes from 10m to 30m. The first two columns plot the input Hermite Gaussian modes and final field. The third column plots the free propagation of each input mode over 20m. The modes in the second column deviate from both the first and third column indicating interaction with electron beam. Power amplification for each Hermite Gaussian mode is plotted in Fig. 7. For 10m to 30m, where is the linear regime, the fundamental mode has the strongest coupling to the electron beam and therefore the maximal power gain. Therefore the transverse distribution of electric field is able to maintain a Gaussian like distribution in linear regime. For the post saturation regime, e.g. from 50m to 70m, higher order modes $HG_{1,0}$ and $HG_{0,1}$ have stronger coupling to the electron beam than the fundamental mode (Fig. 7). This agrees with the increase of ratio of high order mode we find out in mode decomposition as FEL proceed to post saturation.

HG'_n is then decomposed into Hermite-Gaussian mode,

$$\hat{O}_{FEL}\phi_n = \sum \alpha_{pn} \phi_p. \quad (8)$$

Eigenmodes of \hat{O}_{FEL} can then be computed from this $\{\alpha\}$ matrix. Assuming the q th eigenmode is defined as $\sum \beta_n^q \phi_n$,

$$\hat{O}_{FEL} \sum_n \beta_n^q \phi_n = \lambda^q \sum_n \beta_n^q \phi_n \quad (9)$$

$$= \sum_{n,p} \beta_n^q \alpha_{pn} \phi_p. \quad (10)$$

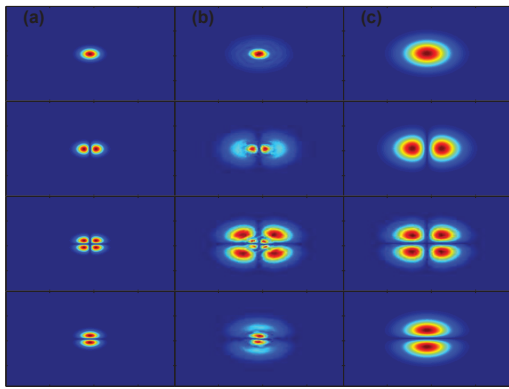


Figure 6: Column(a) plots the input Hermite Gaussian modes at the entrance of the undulator section. Column(b) plots the resultant field for each Hermite Gaussian mode at the end. Column(c) plots the free propagation result across the same distance as a comparison.

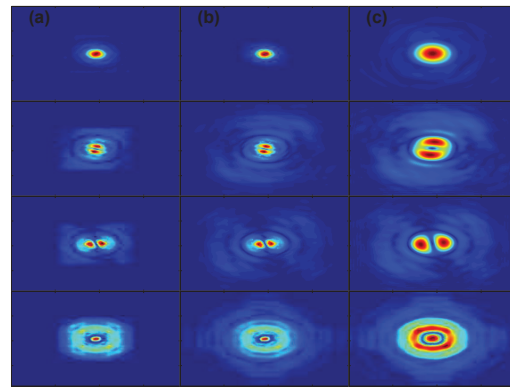


Figure 8: Column (a) plots the eigenmodes at the entrance of the undulator. Column (b) plots output field at the end of the undulator for each mode respectively. Column (c) shows the free propagation result across the same distance for each eigenmode.

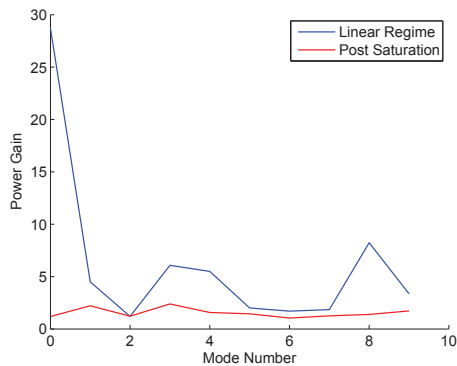


Figure 7: Power gain is computed by dividing the power of the input mode HG_n by the power of the output mode HG'_n .

Since \hat{O}_{FEL} is a non-self-adjoint operator, $\{\beta^q\}$ are not orthogonal vectors and $\{\lambda^q\}$ are complex eigenvalues. Fig. 8 plots the first four eigenmodes for the \hat{O}_{FEL} from $15m$ to $25m$. The first mode is a Gaussian like mode. The second and third mode are dipole mode like, and with different orientations. The fourth mode is azimuthal symmetric and has one node in radial direction. The first and fourth mode are usually found as the first and second mode in 3D FEL theory. In these theories, mostly an azimuthal symmetry in electric field is assumed. In our simulation, we are able to find modes that break this symmetry since the Hermite Gaussian basis has this degree of freedom. As a comparison, we plot the interaction of these eigenmodes with electron bunch and their free propagation results for the same distance. Eigenmodes maintain their distribution through interaction with electron beam. If the eigenmodes are propagated freely across the same distance, as is shown in column (c), distribution will be strongly diffracted.

CONCLUSION

In this paper, we propose a mode decomposition method using Hermite Gaussian mode as basis. We find that there are some region of w , within which the orthogonal condition is well satisfied. Wavefront curvature R is fitted by free propagation method. And w is chosen such that the fundamental Gaussian mode has the most dominating power. With this method, we are able to analyze mode component in different regimes. The fundamental mode is found to maintain a good portion of power in a tapered FEL. Coherence function is computed using the decomposed mode amplitude. Mode evolution is also studied based on this method. The eigenmodes of the FEL operator is computed by simulating Hermite Gaussian mode interacting with electron beam individually.

ACKNOWLEDGMENT

The authors would like to thank Professor S.-Y. Lee of Indiana University for many stimulated discussions. K.F. would like to express his gratitude to Prof. Lee for many advices. The work was supported by the US Department of Energy (DOE) under contract DE-AC02-76SF00515 and the US DOE Office of Science Early Career Research Program grant FWP-2013-SLAC-100164. The work of K.F. was also supported by the US DOE grant DE-FG02-12ER41800 and National Science Foundation grant NSFPHY-1205431.

REFERENCES

- [1] H.N. Chapman, P. Fromme, A. Barty, T.A White, R.A. Kirian, A. Aquila, M.S. Hunter, J. Schulz, D.P. DePonte, U. Weierstall, R.B. Doak, F.R.N.C. Maia, A. Martin, I. Schlichting, "Femtosecond X-ray protein nanocrystallography", *Nature* **470**, 73-78 (2011).
- [2] M.M. Seibert, T. Ekeberg, F.R.N.C. Maia, M. Svenda, J. Andreasson, O. Jönsson, D. Odić, B. Iwan, A. Rocker, D. Westphal, M. Hantke, D.P. DePonte, "Single mimivirus particles

- intercepted and imaged with an X-ray laser”, *Nature* **470**, 78-81 (2011).
- [3] N.M. Kroll, P.L. Morton, M.R. Rosenbluth, “Free-Electron Lasers with Variable Parameter Wigglers”, *IEEE J. Quantum Electron.*, **QE-17**, 1436-1468 (1981).
- [4] X. Wang, H. Freund, D. Harder, W. Miner, J. Murphy, H. Qian, Y. Shen, and X. Yang, “Efficiency and Spectrum Enhancement in a Tapered Free-Electron Laser Amplifier”, *Phys. Rev. Lett.* **103**, 154801 (2009).
- [5] Y. Jiao, J. Wu, Y. Cai, A.W. Chao, W.M. Fawley, J. Frisch, Z. Huang, H.-D. Nuhn, C. Pellegrini, S. Reiche, “Modeling and multidimensional optimization of a tapered free electron laser”, *Phys. Rev. ST Accel. Beams*, **15**, 050704 (2012).
- [6] S. Reiche, “GENESIS 1.3: a fully 3D time-dependent FEL simulation code”, *Nucl. Instrum. Methods A*, **429**, 243 (1999).
- [7] J. Wu and L.H. Yu, “Eigenmodes and mode competition in a high-gain free-electron laser including alternating-gradient focusing”, *Nucl. Instrum. Methods A*, **475**, 79-85 (2001).